Supporting Information

Painter et al. 10.1073/pnas.0913139107

SI Text

Basin Description. The headwaters of the Colorado River Basin lie in the Rocky Mountains of Colorado, Wyoming, and Utah (Fig. S1). The Upper Colorado River Basin (UCRB) lies downwind of the Colorado Plateau and the Great Basin physiographic provinces, optimally positioned to receive dust emitted from these regions given the southwesterly flow of deposition events observed in the mountains of the UCRB (1). The eastern half of the basin lies downwind of the yellow and red soils of the Colorado Plateau. The western half generally lies downwind of the predominantly yellow soils of the Great Basin. Ultimately, quantification of the spectral absorptivity (color) of these soils will be an important component of an integrated desert-mountain model.

The land cover for the UCRB from the National Land Cover Database (2) is mapped in Fig. S2, overlain with the Variable Infiltration Capacity (VIC) one-eighth degree resolution model grid. In general, the regions of greater snow accumulation lie in the forest (subalpine) or barren (alpine) classes at elevations above 1,800 m. Due to the resolution of the model grid, the majority of grid cells, even at high elevations, contain some fraction of forest canopy cover. The UCRB receives an area-averaged 405 mm/y of precipitation and drains 29 million hectare of largely semiarid landscape above Lees Ferry, AZ. Although the average annual runoff over 1916–2003 was 18.3 bcm, reconstructions of flow indicate that the long-term flow lies in the range 17.7–18.1 bcm (3, 4).

Unlike the Upper Basin states, the Lower Basin states fully use their allocations. Recent concerns over Lower Basin long-term use of unused Upper Basin water and a major drought led to two recent landmark agreements that address surpluses (in 2001) and shortages (in 2007). The 5% of flow lost due to radiative forcing by dust is a large proportion of Lower Basin municipal use, representing twice the annual allocation of Las Vegas (0.37 bcm, 0.30 maf), and 50% more than the basic annual allocation for the Los Angeles metropolitan area (0.68 bcm, 0.55 maf).

VIC Hydrological Model. The same meteorological inputs of precipitation, maximum and minimum temperature, and wind speed were used as in ref. 5, as were the physical characteristics of the basin (i.e., terrain, soil depth, vegetation type, and coverage). Snow processes are configured in a two-layer snow system within five snow elevation bands, to improve representations of snow accumulation in areas with rough topography. Land cover is represented with a subgrid mosaic, allowing multiple, fractional cover types per cell. Canopy interception and throughfall of precipitation vary with vegetation type. Energy and moisture fluxes in each grid cell are calculated for a three-layer soil system, with baseflow calculated empirically from the moisture content in the lowest soil layer. Infiltration and runoff are determined using the variable infiltration curve, which describes the subgrid variability in soil moisture. Each grid cell is treated as a level surface and is evaluated for the full time period independently, and streamflow is simulated via a postprocessing step that routes runoff and baseflow from individual cells through a stream network.

Albedo Parameterizations. Dust and soot are more absorptive of solar radiation in the visible and near-infrared wavelengths than ice and snow (1, 6, 7). When these impurities lie in near surface layers, they absorb incident solar radiation and transfer this energy to the surrounding snow grains largely through conduction. In a snow cover that is below 0 °C, this absorbed radiation warms the snow column and, once the snow temperature reaches 0 °C, the additional absorbed radiation contributes to melt. As mentioned in the main text, the increase in snow surface temperature and more frequent melting of the surface increase the saturation vapor pressure at the snow surface, increasing sublimation and evaporation.

In Fig. S3*A*, we show the range of albedos under accumulation (solid) and melt (dashed) conditions for the after disturbance dust loading (ADL) parameterization across 30 d (red; used in the historical base run of VIC), the before disturbance dust loading (BDL) parameterization across 30 d (blue), and that for clean snow under accumulation and melt conditions (black). The clean snow parameterizations shown here (Fig. S3 *A*) are based on results in ref. 8.

The following describes how the parameterizations are handled. No instantaneous dust events occur in the model. Rather, a snowfall event returns snow age to 0 and the snow albedo ages according to elapsed days since this snowfall. The aging is more aggressive in the ADL scenarios than in the BDL scenarios. Likewise, the aging is more aggressive in the ablation period than the accumulation period because of the greater dust loading during that period and more rapid snow metamorphism and grain growth.

The BDL scenario does not include changes in atmospheric scattering and absorption associated with a lesser atmospheric dust loading because there is great uncertainty and spatial heterogeneity in the net forcing from scattering and absorption of aerosols (9, 10). Moreover, the dust storms that produce the loading to the UCRB are markedly episodic, whereas dust's presence and radiative forcing in snow surface layers is sustained and increases with snowpack ablation as buried dust layers emerge on the surface (1).

Discussion. Though the peak discharge is lower under the current ADL conditions than under BDL, the rising limb of the ADL hydrograph is steeper (Fig. 2*A*). Therefore, accelerated melt from dust and this steeper rising limb induces stress in current water management in the Colorado River Basin (CRB) at a range of scales. Recall that water management has always been subject to this stress because water management began in the CRB in the 20th century, after dust forcing reached its modern levels. A reduction in dust loading would reduce present system stress and recover lost runoff.

In spring 2009, dust emission into the UCRB reached the highest levels in our period of observation of dust deposition (2003–2009) and by far the greatest in memory according to anecdotal reports from water managers and mountain residents. Its impact was widely felt by reservoir managers who saw dramatic melt rates and far earlier than normal peak runoff, necessitating unprecedented early releases and rapid responses. Many of the management decisions were informed by qualitative dust in snow advisories produced collaboratively by the Center for Snow and Avalanche Studies, the Snow Optics Laboratory at the Jet Propulsion Laboratory, and the National Snow and Ice Data Center under the Colorado Dust-On-Snow program. Estimates of dust impacts on runoff thus have immediate water management implications in addition to longer-term planning ramifications, and management interests would stand to benefit from a quantitative dust impact forecasting capability.

1. Painter TH, et al. (2007) Impact of disturbed desert soils on duration of mountain snow cover. *Geophys Res Lett* 34, 10.1029/2007GL030284.
2. Homer C, et al. (2007) Completion of the 2001 National Land Cover Database for the conterminous United States. *Photogramm Eng Rem S* 73:337–341.
3. Meko DM, et al. (2007) Medieval drought in the upper Colorado River Basin. *Geophys Res Lett* 34, 10.1029/2007GL029988.
4. Woodhouse CA, Gray ST, Meko DM (2006) Updated streamflow reconstructions for the Upper Colorado River Basin. *Water Resour Res* 42, 10.1029/2005WR004455.
5. Hamlet AF, Mote PW, Clark MP, Lettenmaier DP (2007) Twentieth-century trends in runoff, evapotranspiration, and soil moisture in the Western United States. *J Climate* 20:1468–1486, 10.1175/JCLI4051.1.
6. Flanner MG, et al. (2009) Springtime warming and reduced snow cover from carbonaceous particles. *Atmos Chem Phys* 9:2481–2497.
7. Hansen J, Nazarenko L (2004) Soot climate forcing via snow and ice albedos. *Proc Natl Acad Sci USA* 101:423–428.
8. Flanner M, Zender C (2006) Linking snowpack microphysics and albedo evolution. *J Geophys Res* 111, 10.1029/2005JD006834.
9. Ramanathan V, et al. (2007) Warming trends in Asia amplified by brown cloud solar absorption. *Nature* 448:575–578, 10.1038/nature06019.
10. Kim J, Gu Y, Liou KN (2006) The impact of direct aerosol radiative forcing on surface insolation and spring snowmelt in the southern Sierra Nevada. *J Hydrometeorol* 7:976–983.
11. Davis RE, Nolin AW, Jordan R, Dozier J (1993) Towards predicting temporal changes of the spectral signature of snow in visible and near-infrared wavelengths. *Ann Glaciol* 17:143–148.
12. Nolin AW, Dozier J (2000) A hyperspectral method for remotely sensing the grain size of snow. *Remote Sens Environ* 74:207–216.
13. Painter TH, Dozier J, Roberts DA, Davis RE, & Green RO (2003) Retrieval of subpixel snow-covered area and grain size from imaging spectrometer data. *Remote Sens Environ* 85:64–77.

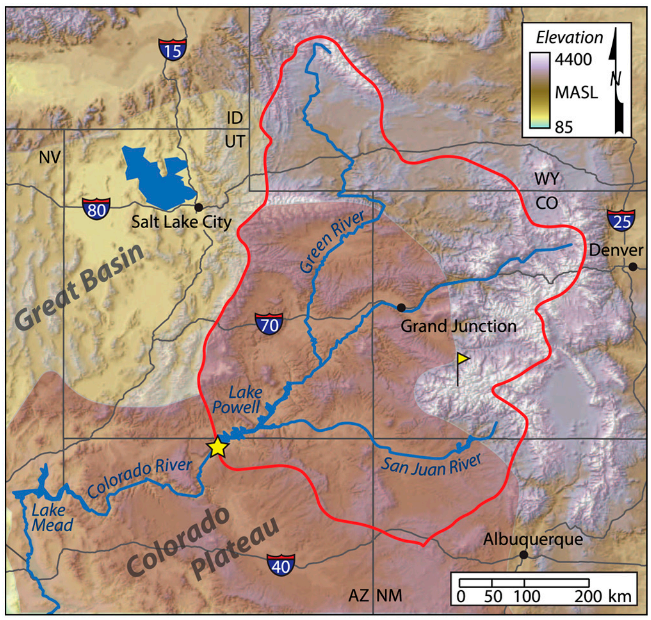

Fig. S1. Elevation map of the Upper Colorado River Basin, outlined in red. Star marks Lee's Ferry, AZ, the dividing point between the Upper and Lower Basins. Flag marks Senator Beck Basin Study Area, in the San Juan Mountains of Colorado, where energy balance modeling and albedo measurements were used to constrain this sensitivity study.

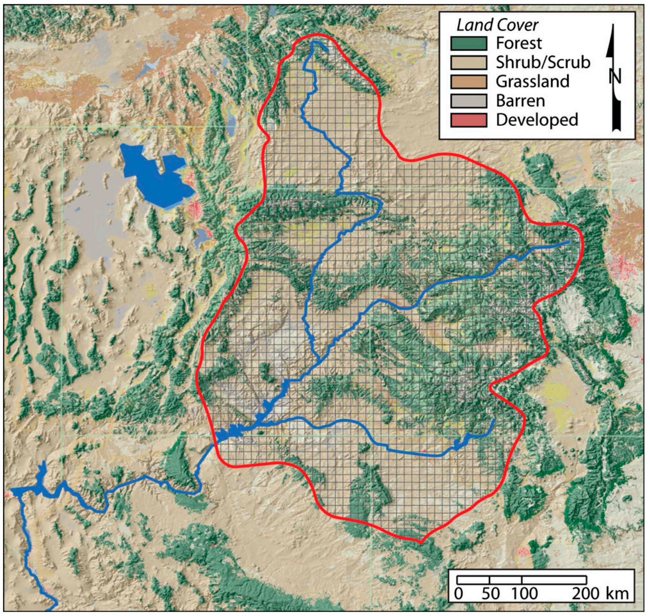

Fig. S2. Land cover of the Upper Colorado River Basin and surrounding region, based on the National Land Cover Dataset (2). The VIC modeling grid is draped on the land cover map to show the spatial distribution of forest, tundra, and bare ground in the UCRB.

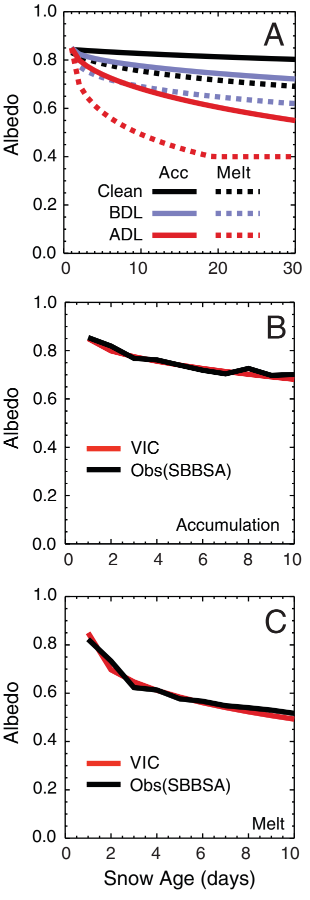

Fig. S3. (*A*) Clean snow, BDL, and ADL albedo age curves for accumulation (T < 0 °C) and melt (T > 0 °C) periods. Clean snow curves are for optical grain sizes ranging from 40 to 200 μm radius (accumulation) and 40 to 800 μm radius (melt) (11–13). (*B*) Comparison of VIC parameterization for accumulation period with measurements from the Senator Beck Basin Study Area (SBBSA) (1). (*C*) Comparison of VIC parameterization for melt period with measurements from the SBBSA (1). The albedo age curves from SBBSA were from the means of three age curves for each period from 2005 and 2006 (1).

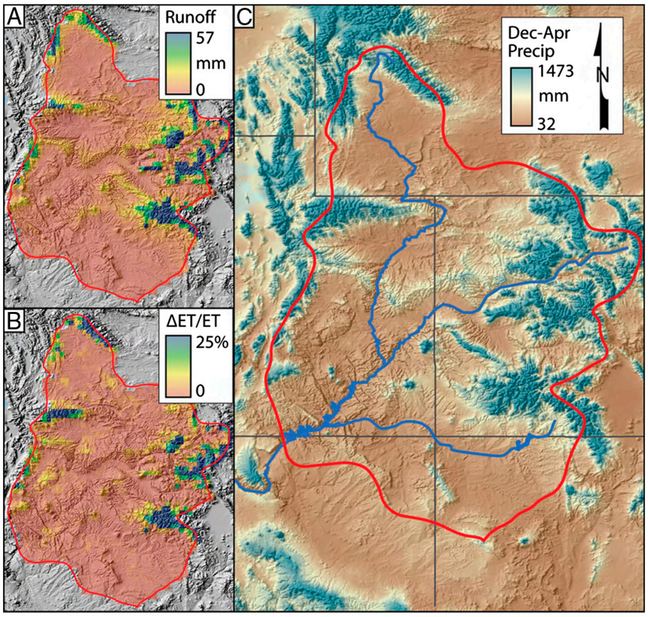

Fig. S4. (*A*) Time-averaged total annual runoff for ADL scenario across Upper Colorado River Basin, averaged across 1916–2002. (*B*) Annual change in evapotranspiration (ET) between BDL and ADL relative to total ET for ADL across the UCRB, averaged across 1916–2002. (*C*) Annual average precipitation across the UCRB. These data show that the greatest impact on ET occurs in those regions of the greatest contribution of runoff to the river: the mountains.

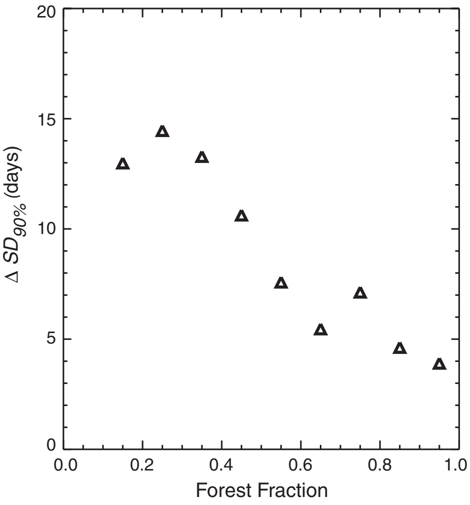

Fig. S5. Change in date of 90% snow water equivalent ablation, $\Delta SD_{90\%}$, versus forest fraction. This result shows that VIC appropriately reduces solar irradiance with greater forest fraction and thus reduces the capacity of dust to impact snow melt.

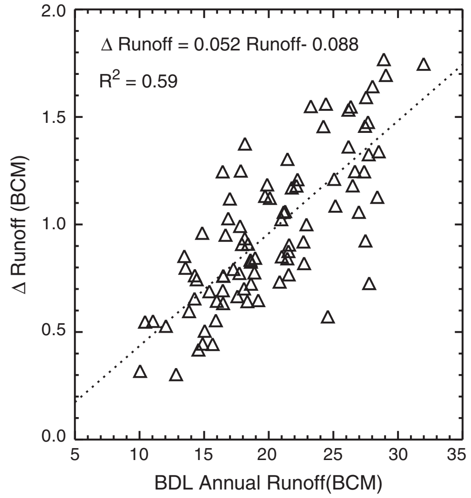

Fig. S6. Δ runoff versus BDL annual runoff (billion cubic meters) for the period of simulation 1916–2003. Each symbol represents an individual year.